ISSN 1070-3284, Russian Journal of Coordination Chemistry, 2013, Vol. 39, No. 1, pp. 147–155. © Pleiades Publishing, Ltd., 2013.

Syntheses, Crystal Structures, and Magnetic Properties for Two Spin-Ladder Complexes Based on Bis(2-Thioxo-1,3-Dithiole-4,5-Dithiolato)Nickelate Monoanion Building Block[1]

H. Zhang[a, b], B. Cai[a], H. B. Duan[c, *], G. J. Yuan[a], F. Xuan[a], and X. M. Ren[a, d, *]

[a] *Department of Applied Chemistry, College of Science, Nanjing University of Technology, Nanjing, 210009 P.R. China*

[b] *Department of Chemistry, Huangshan University, Huangshan, 245041 P.R. China*

[c] *School of Biochemical and Environmental Engineering, Nanjing Xiaozhuang College, Nanjing, 210017 P.R. China*

[d] *Coordination Chemistry Institute and State Key Laboratory, Nanjing University, Nanjing, 210093 P.R. China*

**e-mail: duanhaibao4660@163.com; xmren@njut.edu.cn*

Received July 12, 2011

Abstract—Two isostructural complexes based on bis(2-thioxo-1,3-dithiole-4,5-dithiolato)nickelate monoanion ($[Ni(Dmit)_2]^-$) building block, ($C_{19}H_{11}NNiF_3S_{10}$ (**I**) and $C_{18}H_{10}N_2F_3NiS_{10}$ (**II**)), have been synthesized and characterized structurally and magnetically. Two complexes crystallize in monoclinic space group $P\bar{1}$ with very similar cell parameters and packing structures. The planar $[Ni(Dmit)_2]^-$ monoanions form face-to-face π-type dimer, and the neighboring dimers are aligned into a ladder-type arrangement via lateral-to-lateral S···S contacts along *x* axis in the crystals of **I** and **II**. Two complexes exhibit similar magnetic behaviors, and their magnetic susceptibility data can be fitted to a Heisenberg antiferromagnetic two-legged spin ladder formula in high-temperature region and reproduced well by the Troyer expression in low-temperature region. The spin-gap values, obtained, respectively, from the fits of magnetic susceptibility data in high- and low-temperature regions, are closed to each other, indicating the chose magnetic exchange model and the results of fits are reasonable.

DOI: 10.1134/S1070328412120068

INTRODUCTION

Bis-1,2-dithiolene complexes of transition metal have been widely studied due to their novel properties and applications in the areas of conducting and magnetic materials, dyes, non-linear optics, catalysis and others [1–9]. Experimental and theoretical investigations indicated that these applications arise from the specific geometries and intermolecular interactions of bis-1,2-dithiolene complex anions and the materials properties are hypersensitive to the anions stacking pattern [1, 2]. In our previous studies, a series of quasi-one-dimensional (quasi-1D) quantum magnetic chain systems have been built using bis(maleonitriledithiolato)nickelate monoanion $[Ni(Mnt)_2]^-$ as the magnetic architecture and benzylpyridinium derivative as the countercation, among them, a novel spin-Peierls-type transition (a magnetic transition from paramagnetic to nonmagnetic phases) below a critical temperature was observed in some complexes [10–16].

Most recently, we have being devoted our research to the molecular magnets self-assembled from magnetic bis(l,3-dithiole-2-thione-4,5-dithiolate)nickelate monoanion ($[Ni(Dmit)_2]^-$) architecture owing to its molecular and electronic structures resemble to those of $[Ni(Mnt)_2]^-$ ion. The $[Ni(Dmit)_2]^-$ ion is also an excellent building block employed for constructing molecular magnetic materials apart from its well-known electric conductivity. In comparison with $[Ni(Mnt)_2]^-$ complexes, the presence of versatile S···S interaction manners in $[Ni(Dmit)_2]^-$ complexes lead to adaptable arrangements between the neighboring $[Ni(Ddmit)_2]^-$ anions in the crystal, for instance, the styles of cofacial stack, lateral-to-lateral or head-to-tail S···S contacts between the neighboring $[Ni(Dmit)_2]^-$ anions, which could give rise to 1D chain [17], 1D ladder [18, 19] or 2D layer [20, 21] arrangements of $[Ni(Dmit)_2]^-$ anions, are generally observed. Diverse stacking structures of $[Ni(Dmit)_2]^-$ anions maybe give differently physical properties of materials. Working along these lines, two complexes with 1D laddered arrangements of $[Ni(Dmit)_2]^-$ anions have been achieved via introducing the benzylpyridinium derivatives into $[Ni(Dmit)_2]^-$ spin systems. It is fascinating that one complex (with lateral-to-lateral S···S contacts between the neighboring $[Ni(Dmit)_2]^-$ anions within the laddered-type chain) exhibits long-

[1] The article is published in the original.

range antiferromagnetic (AFM) ordering, whereas another complex (with head-to-tail S···S contacts between the neighboring $[Ni(Dmit)_2]^-$ anions within a laddered-type chain) shows a spin-Peierls-type magnetic transition [22]. Furthermore, three polymorphs with 2D layered arrangements of $[Ni(Dmit)_2]^-$ anions were obtained, replacing benzylpyridinium derivative by a benzylquinolinium derivative, and these polymorphs show unusual behavior of spin bistability with bigger hysteresis loop (~50 K) [23].

In order to gain an insight into the correlations between the molecular structure of the countercation and the arrangement of $[Ni(Dmit)_2]^-$ anion as well as the correlations between the magnetic behavior of the molecular solid and the arrangement of $[Ni(Dmit)_2]^-$ anion, we are systematically exploring the series of $[Ni(Dmit)_2]^-$ complexes. Herein, we present the investigations of the crystal structures and magnetic properties for two new spin-ladder complexes of $[Ni(Dmit)_2]^-$ monoanion with 1-N-(4'-trifluoromethylbenzyl)pyridinium and 1-N-(4'-trifluoromethylbenzyl)pyrazinium, respectively, ($C_{19}H_{11}NNiF_3S_{10}$ (**I**) and $C_{18}H_{10}N_2F_3NiS_{10}$ (**II**)).

EXPERIMENTAL

Chemicals, reagents, and materials. All chemicals and solvents were reagent grade and used as received. Tetrabutylammonium bis(1,3-dithiol-2-thione-4,5-dithiolato)nickelate ($[Bu_4N][Ni(Dmit)_2]$) was synthesized following the reported method in [24]. The complexes, 1-N-(4'-trifluoromethylbenzyl)pyridinium bromide ([4'-CF_3-BzPy]Br) and 1-N-(4'-trifluoromethylbenzyl)pyrazinium bromide ([4'-CF_3-BzPy]Br) were prepared utilizing a routine literature procedure [22, 23].

Synthesis of I and II. The procedures for preparing **I** and **II** are similar to each other, and the general process of preparation is described below, the equivalents of $(Bu_4N)[Ni(Dmit)_2]$ and [4'-CF_3-BzPy]Br for **I**, and [4'-CF_3-BzPz]Br for **II** dissolved in acetonitrile are mixed at room temperature, the immediately formed precipitate was separated and dried in vacuum. The yield was ~60%. The precipitate is then re-dissolved in acetone. As the acetone solution evaporated slowly at room temperature, the plate-like dark-green crystals, which are suitable for X-ray diffraction, were obtained after 5–7 days.

For $C_{19}H_{11}NNiF_3S_{10}$ (**I**)

anal. calcd., %:	C, 33.09;	N, 2.03;	H, 1.61.
Found, %:	C, 32.88;	N, 2.18;	H, 1.86.

IR spectrum (KBr disc; ν, cm^{-1}): 3049 w (ν(C–H) of phenyl or pyridyl ring); 2974 w and 2924 w (ν(C–H) of $-CH_2-$ group); 1613 sh, 1485, 1444, 1417 and 1385 (ν(C=C) or ν(C=N) of the phenyl or pyridyl ring); 1349 s (ν(C=C) of $Dmit^{2-}$ ligand); 1159 s and 1117 s (symmetric and asymmetric C–F stretch of $-CF_3$ group); 1061 s (ν(C=S) of $Dmit^{2-}$ ligand).

For $C_{18}H_{10}N_2F_3NiS_{10}$ (**II**)

anal. calcd., %:	C, 31.30;	N, 4.06;	H, 1.46.
Found:	C, 31.09;	N, 3.95;	H, 1.52.

IR spectrum (KBr disc; ν, cm^{-1}): 3012 w (ν(C–H) of phenyl or pyridyl ring); 2967 w, 2925 w (ν(C–H) of $-CH_2-$ group); 1604 sh, 1440, and 1385 s (ν(C=C) or ν(C=N) of the phenyl or pyridyl ring); 1350 s (ν(C=C) of $Dmit^{2-}$ ligand); 1161 s and 1124 s (symmetric and asymmetric C–F stretch of $-CF_3$ group); 1061 s (ν(C=S) of $Dmit^{2-}$ ligand).

Physical measurements. Elemental analyses for C, H, and N were carried out with a PerkinElmer 240 analytical instrument. IR spectra (KBr pellets) were collected by a Fourier Transform Infrared spectrophotometer (170SX) in the range of 4000–400 cm^{-1}. Magnetic susceptibilities of **I** and **II** were collected on microcrystalline samples from 1.8 to 300 K under a magnetic field of 1000 Oe, using a Quantum Design MPMS-XL SQUID magnetometer.

X-ray crystallography. Single crystals of **I** and **II** suitable for X-ray diffraction study were, respectively, selected and mounted on a glass capillary, and the diffraction intensity data were collected at 293 K (or 296 K) by a Bruker AXS SMART diffractometer equipped with CCD area detector and MoK_α (λ = 0.71073 Å) radiation [25]. The structures of **I** and **II** were solved using direct method and refined with the SHELX-97 [26] by the full-matrix least-squares procedure on F^2, respectively. All non-hydrogen atoms were refined anisotropically and the hydrogen atoms were introduced at calculated positions. The trifluoromethyl group exhibits disorder in the crystal structures of both **I** and **II**, and each fluorine atom has two sites, which occupation factor was refined. The crystallographic details about data collection and structure refinements for **I** and **II** are summarized in Table 1. Supplementary material for structure **I** and **II** has been deposited with the Cambridge Crystallographic Data Centre (no. 802392 (**I**) and 802393 (**II**); deposit@ccdc.cam.ac.uk or http://www. ccdc.cam.ac.uk).

Table 1. Crystallographic data and refinement parameters for complexes **I** and **II**

Parameter	Value	
	I	**II**
Formula weight	689.60	690.59
Crystal system	Triclinic	Triclinic
Space group	$P\bar{1}$	$P\bar{1}$
a, Å	9.3400(16)	9.3068(7)
b, Å	11.847(2)	11.8007(9)
c, Å	12.102(2)	11.8419(8)
α, deg	97.739(2)	97.1010(10)
β, deg	91.227(2)	91.4030(10)
γ, deg	103.538(2)	102.6990(10)
V, Å^3; Z	1288.2(4); 2	1257.22(16); 2
ρ_{calcd}, g cm^{-1}	1.778	1.824
F(000)	694	694
μ, mm^{-1}	1.598	1.638
θ Ranges, deg	1.70–25.50	1.74–25.50
Index ranges	$-11 \le h \le 11$, $-14 \le k \le 14$, $-14 \le l \le 13$	$-10 \le h \le 11$, $-14 \le k \le 14$, $-6 \le l \le 14$
Reflections collected	9476	6883
Independent reflections	4715	4643
Observed data, $I > 2\sigma(I)$	3605	3708
R_{int}	0.0271	0.0364
Parameters	336	335
Goodness of fit on F^2	1.060	0.966
Final R indices ($I > 2\sigma(I)$)*	$R_1 = 0.0352$, $wR_2 = 0.0869$	$R_1 = 0.0312$, $wR_2 = 0.0757$
R indices (all data)*	$R_1 = 0.0488$, $wR_2 = 0.0961$	$R_1 = 0.0406$, $wR_2 = 0.0791$
Largest diff. peak and hole, e Å^{-3}	0.326/–0.385	0.432/–0.377

* $R_1 = \Sigma\|F_o| - |F_c\|/|F_o|$, $wR_2 = \left[\sum w\left(\sum F_o^2 - F_c^2\right)^2 \Big/ \sum w\left(F_o^2\right)^2\right]^{1/2}$.

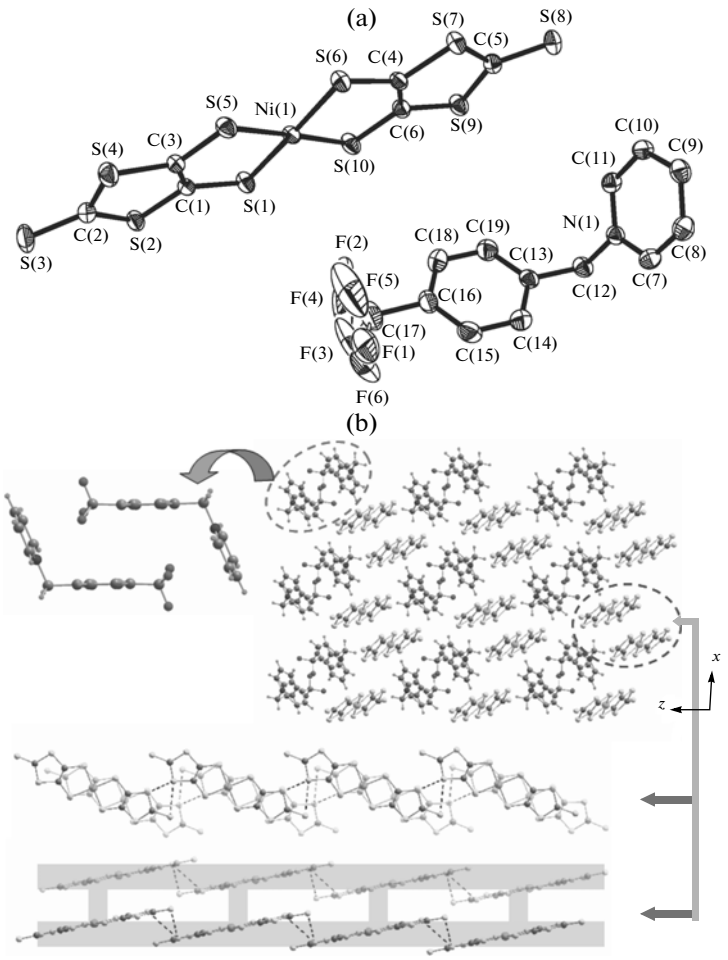

Fig. 1. ORTEP view with non-hydrogen atomic numbering scheme and the thermal ellipsoids at the 30% probability level, all hydrogen atoms omitted for clarity (a) and packing diagram projected along *y* axis which shows a chair-type cation dimer and an anion ladder-type chain formed via lateral-to-lateral S···S contacts for **I** (b).

RESULTS AND DISCUSSION

Complex **I** crystallizes in triclinic space group $P\bar{1}$ with one $[Ni(Dmit)_2]^-$ anion and one cation in an asymmetric unit (Fig. 1a). The $[Ni(Dmit)_2]^-$ monoanion shows an approximately planar geometry, in which the Ni–S distances range from 2.1528(9) to 2.1693(8) Å and two SNiS bite angles are 92.85(3)° and 93.58(3)°. These geometric parameters are comparable to the reported $[Ni(Dmit)_2]^-$ complexes [22, 23]. The 4'-CF_3-$BzPy^+$ cation shows a Λ-shape conformation with a dihedral angle of 68.04° between the phenyl and pyridyl rings; the phenyl and the pyridyl rings make a dihedral angle of 51.79° and 63.88° with the reference plane, N(1)C(12)C(13). It is noted that the trifluoromethyl group shows structurally disorder with two sites for each fluorine atom, the site occupancy factor was refined as 0.61 for F(1), F(2), and F(3) atoms and 0.39 for F(4), F(5), and F(6) atoms.

Two neighboring anions form a face-to-face π-type dimer with the distance of 3.631 Å between the mean molecular planes (which are defined by four coordinated S atoms), and such types of π-type dimers are arranged into a ladder-type chain via lateral-to-lateral S···S contacts with the shorter S···S separations of S(7)···S(2)$^{\#1}$ 3.471 and S(7)···S(3)$^{\#1}$ 3.562 Å (the symmetric code: $^{\#1}$ x, $-1 + y$, z) along crystallographic *y* axis direction (Fig. 1b), whilst the shortest S···S contact, S(5)···S(5)$^{\#2}$ (symmetric code: $^{\#2}$ $1 - x$, $1 - y$, $-z$), is 3.840 Å between two nearest neighboring ladder-type anion chains. Obviously, this distance is larger than the sum of van der Waals radii of two S atoms (3.6 Å) [27]. Two adjacent cations are adopted a chair-type alignment to form a cationic dimer, as demonstrated in Fig. 1b. Their phenyl rings are parallel to each other with a plane-to-plane distance of 4.087 Å. Such kinds of cation dimers fill in the space between the spin ladders, and there only exist weak

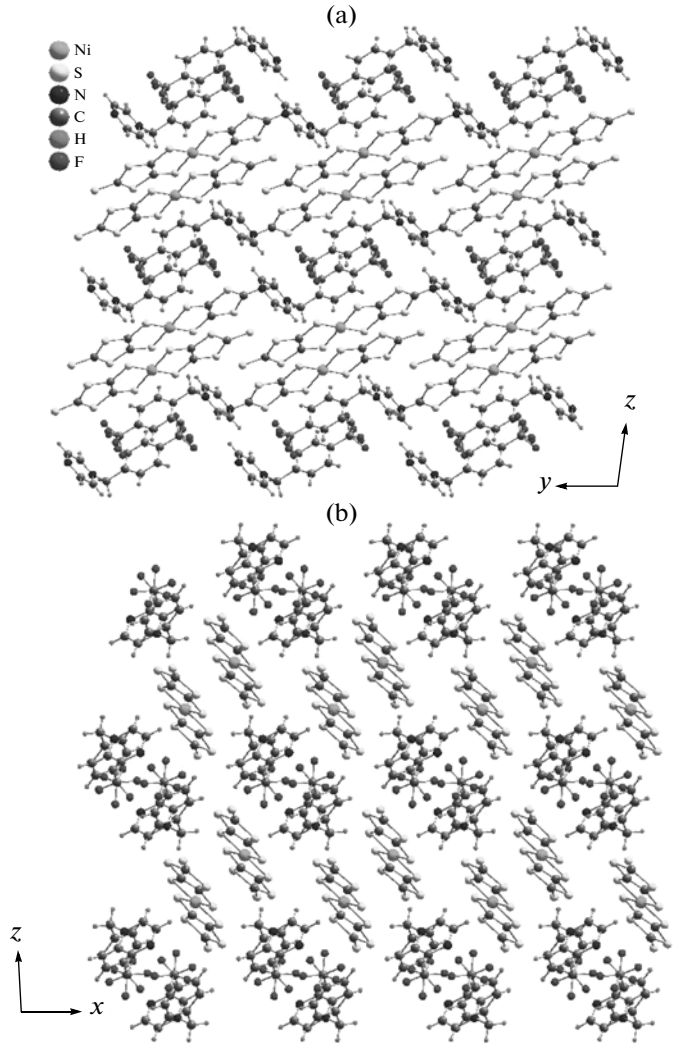

Fig. 2. Packing diagrams for **II** projected along *x* axis (a) and *y* axis (b).

van der Waals forces between the adjacent anions and cations besides electrostatic attraction.

Complex **II** is isostructural with **I**. Two complexes exhibit very similar cell parameters (Table 1, Fig. 2) and packing structures. The molecular structure of **II** is displayed in Fig. 3a. The bond lengths and bond angles in the planar $[Ni(Dmit)_2]^-$ moiety, summarized in Table 2, are normal. The characteristic dihedral angles in the Λ-shape 4'-CF_3-$BzPz^+$ cation are 70.14° between the phenyl and pyrizyl rings as well as 81.42° and 86.76° between the phenyl, the pyrizyl rings with the reference plane, N(1)C(11)C(12), respectively. It is similar to **I** that the anions form the ladder-type chain along crystallographic *y* axis via face-to-face stack (with the distance of 3.576 Å between the mean molecular planes defined by four coordinated S atoms) and lateral-to-lateral S···S contacts (with the shorter S···S separations of S(7)···S(2)$^{\#1}$ 3.515 Å (the symmetric code: $^{\#1}$ $x, -1+y, z$), which is shown in Fig. 3b.

The plots of χ_m as a function of temperature are displayed in Fig. 4 for **I** and **II**, where χ_m represents the molar magnetic susceptibility of one $[Ni(Dmit)_2]^-$ monoanion per formula unit. Two complexes show a similar magnetic behavior, namely, the χ_m value of **I** and **II** gradually decrease in the temperature range of 75–300 K, indicating the existence of a spin gap, while increases below ~60 K upon cooling. The typical Curie paramagnetic behavior of **I** and **II** in low temperature region arises from the magnetic impurity caused by the lattice defects.

From the viewpoint of crystal structure, the magnetic exchange interaction is stronger in a face-to-face stacking π-type $[Ni(Dmit)_2]_2^{2-}$ dimer than a lateral-to-lateral aligning $\left[Ni(Dmit)_2\right]_2^{2-}$ dimer within a lad-

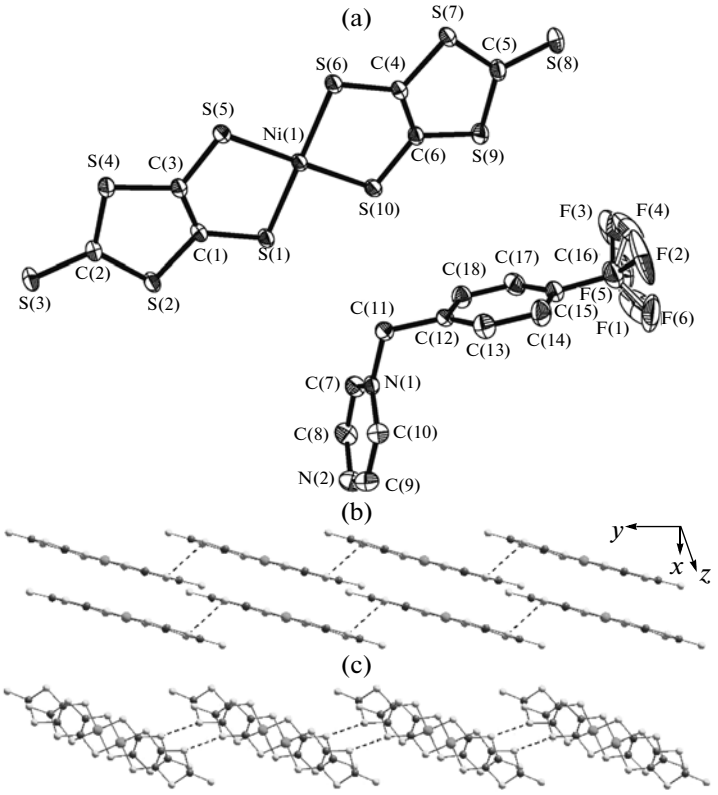

Fig. 3. ORTEP view with non-hydrogen atomic numbering scheme and the thermal ellipsoids at the 30% probability level, all hydrogen atoms omitted for clarity (a), side (b) and top (c) views of one-dimensional ladder-type arrangement of anions along *y* axis for **II**.

der-type chain, since the magnetic orbitals overlap between two $[Ni(Dmit)_2]^-$ monomers is larger in the former case than in the last case; alternatively, the magnetic exchange interaction between the neighboring ladder-type chains could be ignored owing to the interatomic separations between the adjacent $[Ni(Dmit)_2]^-$ monomers being larger than the sum of their van der Waals atomic radii. As above-thought, two kinds of magnetic exchange models, a simple dinuclear (the face-to-face stacking dimer) or a two-legged spin-ladder, are used to analyze the magnetic properties of **I** and **II**. For a dinuclear magnetic exchange model, the molar magnetic susceptibility as a function of temperature can be expressed as Blaney–Bowers equation, Eq. (1), which is deduced from spin Hamiltonian $\hat{H} = -2J\vec{S}_1\vec{S}_2$, or the modified form, Eq. (2), if the magnetic exchange interactions between the neighboring dimers are further considered:

$$\chi_{\text{dimer}} = \frac{Ng^2\beta^2}{k_BT}\left[3 + \exp\left(\frac{-2J}{k_BT}\right)\right]^{-1}, \quad (1)$$

$$\chi_m = \frac{\chi_{\text{dimer}}}{1 - \left(zJ'/Ng^2\beta^2\right)\chi_{\text{dimer}}}. \quad (2)$$

In Eq. (1) and Eq. (2), the parameters J and zJ' represent the magnetic exchange constants of intradimer (face-to-face stacking dimer) and interdimer, respectively; other symbols have their normal meanings. An then, the variable temperature magnetic susceptibilities of **I** and **II** were, respectively, fitted to the simple dinuclear magnetic exchange formulas Eq. (1′) and Eq. (2′) (where χ_0 is the sum of the core diamagnetism from atoms together with the van Vleck paramagnetic components and the term of C/T represents the Curie-type paramagnetic impurity), while the fits are failed to give the reasonable parameters (Fig. 5), suggesting the two-legged spin-ladder magnetic exchange model is probably better to understand the magnetic properties of **I** and **II**:

$$\chi_m = \chi_{\text{dimer}} + \frac{C}{T} + \chi_0, \quad (1')$$

$$\chi_m = \frac{\chi_{\text{dimer}}}{1 - \left(zJ'/Ng^2\beta^2\right)\chi_{\text{dimer}}} + \frac{C}{T} + \chi_0. \quad (2')$$

Since the magnetic susceptibility exhibit an exponential decay upon cooling (in the region of 75–300 K) to indicate the existence of a spin gap for **I** and **II**, the magnetic behavior in low-temperature region is ex-

pected to be well demonstrated by the Troyer expression (Eq. (3)) for a two-legged spin-ladder system with $S = 1/2$ [28]:

$$\chi_m(spin-ladder) = \frac{\alpha}{T^{\gamma}}\exp\left(-\frac{\Delta}{k_B T}\right), \quad (3)$$

where α is a constant corresponding to the dispersion of the excitation energy, γ is a constant between 0.5 and 1 [29]; and Δ is the finite energy gap in the spin-excitation spectrum. Taking into account the contribution of the core diamagnetism and Curie-type paramagnetism, the magnetic susceptibility data of **I** and **II** in low-temperature region were fitted to Eq. (3′), to give the parameters $\alpha, \gamma, \Delta, C$ and χ_0 of 0.34, 657 K, 0.57, 2.55×10^{-3} emu K mol^{-1} and -3.5×10^{-4} emu mol^{-1} for **I** (corresponding to temperature region of 1.8–143 K) as well as 0.59, 537 K, 0.63, 2.29×10^{-3} emu K mol^{-1} and -5.3×10^{-4} emu mol^{-1} for **II** (corresponding to temperature region of 1.8–138 K):

$$\chi_m = \chi_m(spin-ladder) + \frac{C}{T} + \chi_0. \quad (3')$$

Alternatively, in the high-temperature region, χ_m of a two-legged spin ladder with antiferromagnetic exchange interaction is the function of the exchange interactions along the legs (J) and the rung (J') of the ladder, that can be approximated by Eq. (4), given by Barnes and Riera [18, 30]:

$$\chi_m(spin-ladder) = 0.375\left[T^{-1} - \frac{1}{2}\left(J + \frac{1}{2}J'\right)T^{-2} + \frac{3}{16}JJ'T^{-3}\right], \quad (4)$$

$$\chi_m = \chi_m(spin-ladder) + \frac{C}{T} + \chi_0. \quad (4')$$

The experimental magnetic susceptibility data in high-temperature region were fitted to Eq. (4′) to produce the parameters of $J = 86$ K, $J' = 782$ K and -1.8×10^{-4} emu mol^{-1} (C was fixed as 2.55×10^{-3} emu K mol^{-1}) for **I** (corresponding to temperature range of 143–300 K) versus $J = 19$ K, $J' = 543$ K, $C = 2.4 \times 10^{-3}$ emu K mol^{-1} and -2.5×10^{-4} emu mol^{-1} for **II** (corresponding to temperature range of 138–300 K). Since the spin gap in a Heisenberg antiferromagnetic spin-ladder is related to J and J' as

$$\Delta \approx J' - J + \frac{J^2}{2J'}, \quad (5)$$

the Δ values were further evaluated as 701 K for **I** and 524 K for **II** from their J and J' parameters fitted by the magnetic susceptibility data in high-temperature region, these estimated spin gap values are closed to those calculated from Eq. (3), respectively.

In summary, two isostructural spin-ladder complexes based on bis(2-thioxo-1,3-dithiole-4,5-dithiolato)nickelate monoanion building block have been

Table 2. Characteristic bond lengths and angles in $[Ni(Dmit)_2]^-$ moiety of **I** and **II**

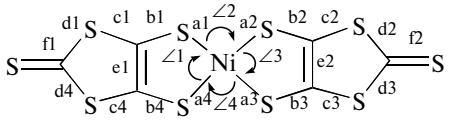

Parameter	Value	
	I	**II**
a1, Å	2.1528(9)	2.1691(6)
a2, Å	2.1625(9)	2.1657(6)
a3, Å	2.1693(8)	2.1552(6)
a4, Å	2.1670(9)	2.1623(6)
b1, Å	1.703(3)	1.723(2)
b2, Å	1.720(3)	1.717(2)
b3, Å	1.723(3)	1.707(2)
b4, Å	1.716(3)	1.721(2)
c1, Å	1.738(3)	1.740(2)
c2, Å	1.744(3)	1.747(2)
c3, Å	1.723(3)	1.740(2)
c4, Å	1.716(3)	1.745(2)
d1, Å	1.721(3)	1.721(2)
d2, Å	1.720(3)	1.728(3)
d3, Å	1.726(3)	1.727(3)
d4, Å	1.740(3)	1.721(2)
e1, Å	1.362(4)	1.348(3)
e2, Å	1.350(4)	1.359(3)
f1, Å	1.643(3)	1.660(2)
f2, Å	1.658(3)	1.644(2)
∠1, deg	92.85(3)	93.51(2)
∠2, deg	86.02(3)	87.41(2)
∠3, deg	93.58(3)	92.93(2)
∠4, deg	87.59(3)	86.15(2)

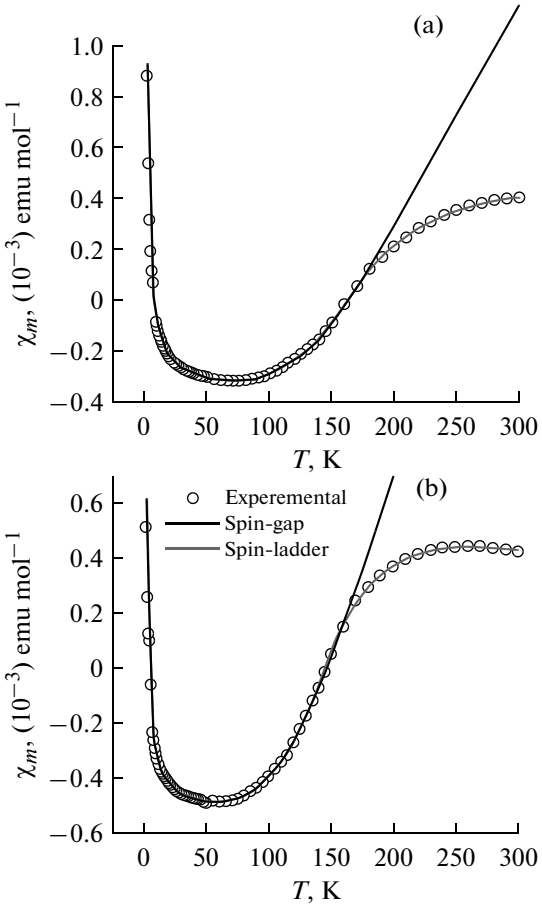

Fig. 4. Plots of χ_M versus T for **I** (a) and **II** (b); open circles: experimental data; lines: fits.

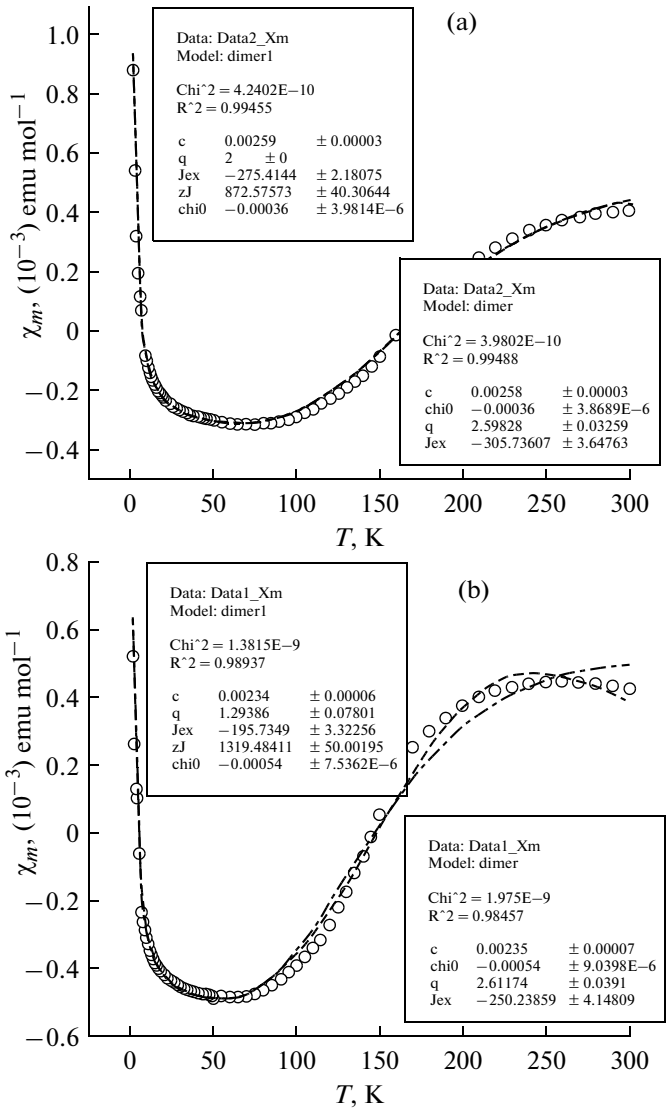

Fig. 5. Magnetic susceptibility, χ_m, as a function of temperature of **I** (a) and **II** (b) (open circles: experimental data; dot lines: fits using a model of isolated spin-dimer and the dimer with magnetic exchange interactions between dimers, respectively).

synthesized and characterized structurally and magnetically. Two complexes show a similar magnetic behavior, the magnetic exchange natures along the legs (J) and the rung (J') of the spin ladder are antiferromagnetic, and the magnetic susceptibility data can be fitted to a Heisenberg antiferromagnetic two-legged spin ladder formula in high-temperature region and reproduced well by the Troyer expression in low-temperature region; the spin-gap values, obtained, respectively, from the fits of magnetic susceptibility data in high- and low-temperature regions, are closed to each other, indicating the chose magnetic exchange model and the results of fits are reasonable.

ACKNOWLEDGMENTS

The authors thank the Natural Science Foundation of High Learning Institutions of Anhui Province, Natural Science Foundation of High Learning Institutions of Jiangsu Province, Postdoctoral Science Foundation of Jiangsu Province and National Nature Science Foundation of China for financial support (grant nos. KJ2012ZD11, 11KJD150004, 1002020B, and 21171097).

REFERENCE

1. Robertson, N. and Cronin, L. , *Coord. Chem. Rev.*, 2002, vol. 227, p. 93.
2. Cassoux, P., *Coord. Chem. Rev.*, 1999, vol. 185, p. 213.
3. Akutagawa, T. and Nakamura, T., *Coord. Chem. Rev.*, 2000, vol. 198, p. 297.
4. Canadell, E., *Coord. Chem. Rev.*, 1999, vol. 186, p. 629.
5. Kato, R., *Chem. Rev.*, 2004, vol. 104, p. 5319.
6. Fourmigué, M., *Acc. Chem. Res.*, 2004, vol. 37, p. 179.
7. Kobayashi, A., Fujiwara, E., and Kobayashi, H., *Chem. Rev.*, 2004, vol. 104, p. 5243.

8. Ouahab, L., *Coord. Chem. Rev.*, 1998, vol. 178, p. 1501.
9. Olk, R.M., Olk, B., Dietzsch, W., et al., *Coord. Chem.* Rev., 1992, vol. 117, p. 99.
10. Duan, H.B., Ren, X.M., and Meng, Q.J., *Coord. Chem.* Rev., 2010, vol. 254, p. 1509.
11. Tian, Z.F., Duan, H.B., Ren, X.M., et al., *J. Phys. Chem. B*, 2009, vol. 113, p. 8278.
12. Tian, Z.F., Ren, X.M., Li, Y.Z., et al., *Inorg. Chem.*, 2007, vol. 46, p. 8102.
13. Ren, X.M., Akutagawa, T., Noro, S., et al., *J. Phys. Chem.* B, 2006, vol. 110, p. 7671.
14. Ren, X.M., Akutagawa, T., Nishihara, S., et al., *J. Phys. Chem.* B, 2005, vol. 109, p. 16610.
15. Dang, D.B., Ni, C.L., Bai, Y., et al., *Chem. Lett.*, 2005, vol. 5, p. 680.
16. Ren, X.M., Meng, Q.J., Song, Y., et al., *Inorg. Chem.*, 2002, vol. 41, p. 5686.
17. Takamatsu, N., Akutagawa, T., Hasegawa, T., et al., *Inorg. Chem.*, 2000, vol. 39, p. 870.
18. Nishihara, S., Akutagawa, T., Hasegawa, T., et al., *Chem. Commun.*, 2002, p. 408.
19. Nishihara, S., Akutagawa, T., Hasegawa, T., et al., *J. Solid. State Chem.*, 2002, vol. 168, p. 661.
20. Kosaka, Y., Yamamoto, H.M., Nakao, A., et al., *J. Am. Chem.* Soc., 2007, vol. 129, p. 3054.
21. Akutagawa, T., Shitagami, K., Aonuma, M., et al., *Inorg. Chem.*, 2009, vol. 48, p. 4454.
22. Chen, Y.C., Liu, G.X., Song, Y., et al., *Polyhedron*, 2005, vol. 24, p. 2269.
23. Zang, S.Q., Ren, X.M., Song, Y., et al., *Inorg. Chem.*, 2009, vol. 48, p. 9623.
24. Steimecke, G., Sieler, H., and Kirmse, J.R., *Phos. Sulfur. Relat. Elem.*, 1979, vol. 7, p. 49.
25. *Bruker, SAINT (version 6.22) and SMART (version 5.625)*, Madison (WI, USA): Bruker-AXS Inc., 2001.
26. Sheldrick, G.M., *SHELXS-97 and SHELXL-97*, Göttingen (Germany): Univ. of Göttingen, 1997.
27. Bondi, A., *J. Phys. Chem.*, 1964, vol. 68, p. 441.
28. Troyer, M., Tsunetsugu, H., and Würtz, D., *Phys. Rev. B*, 1994, vol. 50, p.13515.
29. Johnston, D.C., Kremer, R.K., Troyer, M., et al., *Phys. Rev. B*, 2000, vol. 61, p. 9558.
30. Barnes, T. and Riera, *J., Phys. Rev. B*, 1994, vol. 50, p. 6817.